Check for updates

On the Numerical Determination of the Density and Energy Spatial Distributions relevant for in-Plasma β-Decay Emission Estimation

A. Galatà[1]*, D. Mascali[2], B. Mishra[2,3], E. Naselli[2], A. Pidatella[2] and G. Torrisi[2]

[1]Laboratori Nazionali di Legnaro, Istituto Nazionale di Fisica Nucleare, Legnaro, Italy, [2]Laboratori Nazionali del Sud, Istituto Nazionale di Fisica Nucleare, Catania, Italy, [3]University of Catania, Department of Physics and Astronomy, Catania, Italy

Aim of the PANDORA (Plasmas for Astrophysics, Nuclear Decays Observation and Radiation for Archeometry) project is the in-plasma measurements of decay rates of beta radionuclides as a function of the ionization stage. In this view, a precise calculation of plasma electrons density and energy is mandatory, being responsible for ions' creations and their spatial distribution following plasma neutrality. This paper describes the results of the INFN simulation tools applied for the first time to the PANDORA plasma, including electromagnetic calculations and electrons' dynamics within the so-called self-consistent loop. The distribution of the various electrons' population will be shown, with special attention to the warm component on which depends the obtained ions' charge state distribution. The strict relation of the results with the evaluation of the in-plasma nuclear decays will be also explained.

KEYWORDS

β-decay, plasma traps, numerical simulations, γ-spectroscopy, γ detectors

1 Introduction

Experiments carried out on storage rings demonstrated how the half-life of β-decaying radioactive species could vary considerably when they are in a highly ionized state, compared to the neutral one. In particular, measurements of the half-life of $^{187}Re^{75+}$ ions showed it to be nine orders of magnitude lower compared to the value of 42 Gyr measured for neutral ^{187}Re [1], decaying through bound-state β-decay. In addition, bare ^{163}Dy nuclei, being stable as neutral atoms, become radioactive with a half-life of 33 days [2]. The PANDORA (Plasmas for Astrophysics, Nuclear Decays Observation and Radiation for Archeometry) project Mascali et al. [3] proposes a complementary and challenging approach to measure nuclear β-decays, based on the production of a plasma resembling stellar-like conditions, in order to correlate the decay rate with the thermodynamical properties of the plasma-environment. The study will be

mainly focused on some radionuclides of relevance for Nuclear Astrophysics. To this scope, a compact magnetic trap, based on the Electron Cyclotron Resonance (ECR) principle Geller [4], will be built to confine plasmas of electron densities $n_e \sim 10^{11}–10^{13}$ cm^{-3} or higher and temperatures $kT_e \sim 0.1–30$ keV. By tuning the plasma parameters, it will be possible to establish ion charge state distributions that will mimic specific stellar environments: they will be inferred using an unprecedented set of diagnostics Naselli et al. [5], to which 14 High Purity Germanium (HPGe) detectors will be added to tag the γ-rays accompanying β-decays. In this way, decay rates will be evaluated as a function of the charge state distribution of in-plasma ions Naselli et al. [6]. The total detection efficiency has been estimated through numerical simulations carried out with GEANT4 Agostinelli et al. [7]; Naselli et al. [8], finding values between 0.1% and 0.2% depending on the energy of the γ-rays and supposing a relative efficiency of the detectors of 70%. The HPGe detectors will work in a rather harsh conditions due to the X-rays' and γ-rays' background of about 50 kHz (in each detector, in terms of detected counts per second), self-emitted by the plasma due to the electron bremsstrahlung: this means that each detector should point to an area of the plasma with the highest possible ion density, in order to maximize the counting rate of interest. ECR plasmas are typically far from being uniform, so the knowledge of their fine structure is mandatory: in this view, numerical simulations are a powerful predictive tool to fulfill this task. The two INFN Laboratories, LNL and LNS, have been dedicating their efforts to obtain a self-consistent descritpion of ECR plasmas, by joining precise electromagnetic calculations, carried out with COMSOL-Multiphysics©, with the electrons dynamics calculated with MatLab©. This paper presents the latest results applied to the plasma expected for PANDORA: after a description of the numerical approach adopted in section 2, the calculations portraying the fine structure of the plasma will be shown in section 3, as well as the distribution of electrons in different energy ranges, with a special focus on those relevant for the ionization process. The strict relation of the results with the evaluation of the in-plasma nuclear decays will be discussed in section 4, focusing the attention to the positioning and orientation of the HPGe detectors. Finally, some conclusions will be drawn.

2 The numerical approach

In ECR ion sources and traps a plasma is created by microwaves injected in a cylindrical vacuum chamber, called the plasma chamber, and confined by a particular magnetic structure called "B-minimum", obtained by superimposing the field generated by two or three coils (axial confinement) with the one generated by a sextupole (radial confinement): its characteristic is the production of a field that grows in any

direction, going from the centre of the chamber towards its walls. For the specific case of PANDORA, a fully superconducting magnetic system was chosen, as described in Mauro et al. [9]: the two maxima of the axial field could be tuned between 1.7 and 3 T, the minimum value will be around 0.4 T, while the radial field at the plasma chamber wall will be 1.6 T. The condition for the ECR resonance to take place is that the microwave frequency ω is equal to the electron Larmor frequency $\omega_g = q_e B / 2 m_e$, where q_e and m_e are, respectively, the electron's charge and mass: considering the particular magnetic configuration, this condition is satisfied on specific points forming a closed ellipsoidal-like surface, called resonance surface. Figure 1 shows the resonance surface at 18 GHz (B_{ECR} = 0.64 T) for the typical magnetic configuration that will be used in PANDORA, together with the lateral walls of the plasma chamber: it encloses a volume of less than 3 L (the total value of the plasma chamber being around 44 L).

The frequency used and the geometry of the plasma chamber, working as a resonant cavity, allow the excitation of a given number of resonant modes: compared to the vacuum filled case, the presence of a magnetized plasma modifies the electromagnetic field distribution and the resonant frequencies, through its 3D dielectric tensor that depends (among other parameters) on the plasma density. In particular, the analytical formula implemented in the code is the following:

$$\begin{pmatrix} \epsilon_0 \left(1 - \dfrac{X(1+iZ)}{(1+iZ)^2 - Y^2}\right) & i\epsilon_0 \dfrac{XY}{(1+iZ)^2 - Y^2} & 0 \\[3mm] -i\epsilon_0 \dfrac{XY}{(1+iZ)^2 - Y^2} & \epsilon_0 \left(1 - \dfrac{X(1+iZ)}{(1+iZ)^2 - Y^2}\right) & 0 \\[3mm] 0 & 0 & \epsilon_0 \left(1 - \dfrac{X}{1+iZ}\right) \end{pmatrix} \quad (1)$$

wher $X = (\omega_p/\omega)^2$, $Y = (-\omega_g/\omega)$ and $Z = (\omega_{eff}/\omega)$, being ω_p the plasma frequency and ω_{eff} the collision frequency. From the considerations described above it is clear that simulating the ECR plasma necessitates of a self-consistent approach: in fact, on one hand the electromagnetic field set-up inside the plasma chamber determines, through a resonant interaction, the energetic content of electrons and then the plasma density. On the other hand, the plasma is an anisotropic and dispersive medium characterized by a 3D dielectric tensor, that must be taken into account for the calculation of the electromagnetic field in a kind of self-consistent loop Torrisi et al. [10]. The numerical approach, whose results are presented in this paper, models ECR plasmas by applying an iterative procedure to solve the collisional Vlasov-Boltzmann equation Mascali et al. [11]. By this approach, both an electromagnetic solver, such as COMSOL-Multiphysics© and a kinetic code (written in MatLab©) to solve particles' equation of motion are used in an iterative process, assuming a stationary plasma. The code developed by the two INFN Laboratories, LNL and LNS, has been extensively described elsewhere Galatà et al. [12,13]: it is able to describe both ions and electrons dynamics. In fact, it has been applied to the description of the capture of
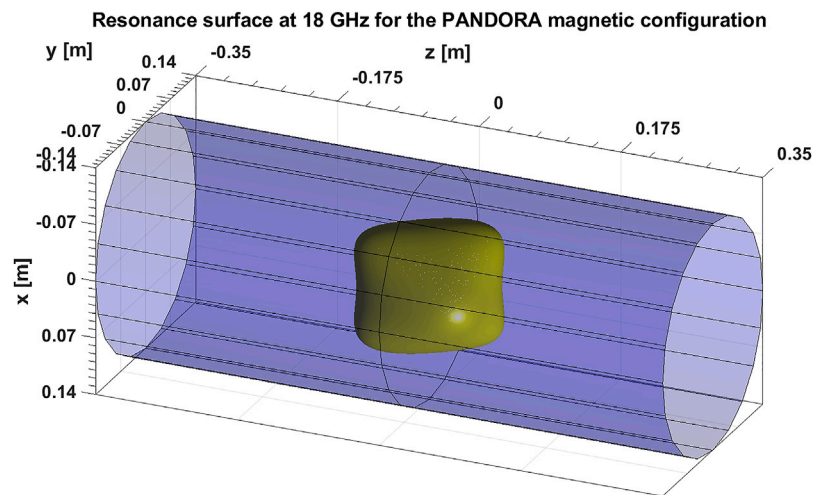
FIGURE 1
Resonance surface at 18 GHz (B_{ECR} = 0.64 T) for the typical magnetic configuration that will be used in PANDORA (in yellow) together with the lateral walls of the plasma chamber (in blue).

externally injected ions by the ECR plasma in the charge breeding process Galatà et al. [14,15], as well as electrons distribution in the ECR source installed at the ATOMKI Laboratory (Hungary), whose results have been used to calculate the characteristic X-rays emitted by an argon plasma Mishra et al. [16]. The domain of the simulation is the portion of the cylindrical plasma chamber between the two maxima of the axial magnetic field (length 700 mm, inner radius 140 mm for the case of PANDORA) and is discretized in cells of 1 mm^3, where COMSOL calculates the electromagnetic field and makes it available for the electrons dynamics as a 3D matrix. It is then loaded by the kinetic code that integrates the electrons equation of motion, including the confining magnetostatic field using the relativistic Boris method Birdsall and Langdon [17] and e-e collisions through the Langevin formalism Manheimer et al. [18]. This formalism is totally equivalent to the solution of the Fokker-Planck equation MacDonald et al. [19]: by supposing plasma particles' velocities being distributed according to a Maxwell-Boltzmann distribution, it is possible to obtain an analytic expression for the so-called coefficient of dynamical friction W_s and the coefficients of parallel and perpendicular diffusion, respectively $D_\parallel$ and $D_\perp$. At each time step of integration T_{step}, the velocity variation $\Delta\mathbf{v}_c$ of a particle as a consequence of Coulomb collisions can then be written as:

$$\Delta\mathbf{v}_c = -W_s\mathbf{v} + \mathbf{v}_{rand} \tag{2}$$

where $\mathbf{v}$ is the instantaneous particle's velocity, the first term on the right side represents the friction, while the second is a random vector taking into account for the build up of a spread in velocity.

The components of this last vector are distributed according to the formula:

$$\phi(\mathbf{v}_{rand}) = \frac{1}{\left(2\pi T_{step}\right)^{3/2} D_\perp D_\parallel^{1/2}} \exp\left(-\frac{v_3^2}{2D_\parallel T_{step}} - \frac{v_1^2 + v_2^2}{2D_\perp T_{step}}\right) \tag{3}$$

where the index "3″ is along the direction of the particle's velocity, while directions one and two are perpendicular to each other and to direction 3. These directions do not necessarily coincide with the spatial coordinates x, y and z, so are identified by the code every T_{step}. By using an ad-hoc routine, the code stores particles' positions and kinetic energies at each time step in 3D matrices reflecting the domain of the simulation, creating "occupation" and "energy accumulation" maps. The occupation maps are opportunely scaled in order to obtain real density maps, while by dividing the energy accumulation map with the occupation map the spatial distribution of the average energy $<sK>$ is obtained. By supposing it belongs to electrons with a Maxwell-Boltzmann (MB) distribution, it is possible to derive the most probable thermal speed c_s, necessary to calculate the various diffusion coefficients, as follow: 1) calculating first the gamma factor using the formula $\gamma = 1 + <K>/mc^2$; 2) then, from the γ factor calculating the average velocity of the MB distribution as $<v> = c \cdot \sqrt{1 - 1/\gamma^2}$; 3) finally, from the average velocity calculating the most probable thermal speed using the formula $c_s = <v> \cdot (\sqrt{\pi}/2)$. Moreover, the code checks also at each T_{step} if the simulated particles are still in the domain of the plasma chamber: if not, particles are removed from the calculation and their positions and
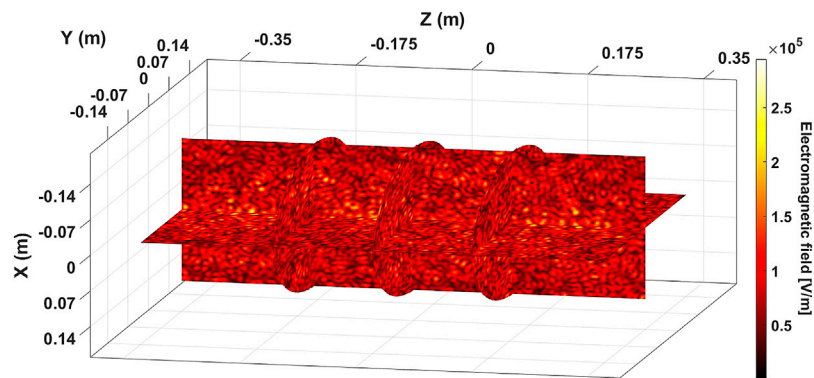
FIGURE 2
Electromagnetic field in vacuum calculated at the end of the Step0.

velocities are stored in the so-called "losses matrix". The applied numerical approach is organized in steps as follows:

- Step0
  1 The electromagnetic field is calculated supposing a vacuum filled cavity, obtaining the field EM_0;
  2 The kinetic code integrates the equation of motion of N electrons uniformly distributed inside the plasma chamber without including the presence of a plasma and under the influence of the external confining magnetic field and EM_0. The output is a real density map $Dens_0$;
- Step1
  1. The map $Dens_0$ is used to derive the plasma 3D dieletric tensor and repeat the electromagnetic calculations including it. The output is a new field EM_1;
  2. The kinetic code integrates the equation of motion of electrons initially distributed as $Dens_0$, without including the presence of a plasma and under the influence of the external confining magnetic field and EM_1. The outputs are a real density map $Dens_{1A}$ and an average energy map $< K_1 >$ or, equivalently, the map of the most probable thermal speed c_{s1};
  3. The kinetic code integrates again the equation of motion, this time of electrons initially distributed as $Dens_{1A}$, including the presence of a plasma (distributed as $Dens_{1A}$ and whose most probable thermal speed is given by the map c_{s1}) through e-e collisions and using EM_1. The output is new real density map $Dens_{1B}$;
- . . .
- Step ith proceeds via the same methodology as presented in Step 1.

The iteration proceeds until the results show self-consistency, that is until the results from consecutive steps show negligible
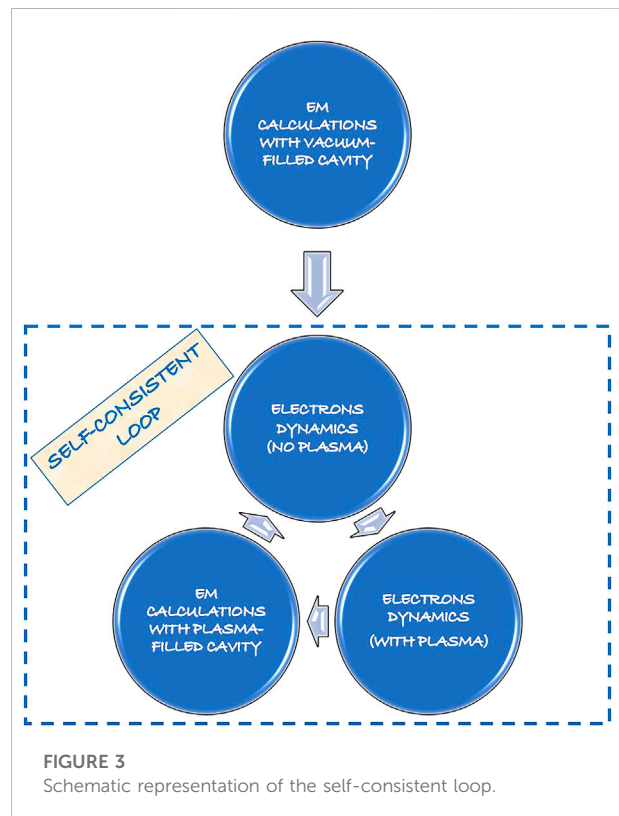
FIGURE 3
Schematic representation of the self-consistent loop.

differences in the density and average energy matrices: this is verified, in particular, by plotting the respective maps, 1D density profiles along the coordinate axes and summing up the density matrices, in order to check if the total number of occupancies stays reasonably constant (within a few percent). As an example, Figure 2 shows the electromagnetic field in vacuum as calculated by COMSOL-Multiphysics© at the end of the Step0:The approach, called self-consistent loop, is schematically

FIGURE 4
1D density profiles along the coordinate axes: **(A)** x direction; **(B)** y direction; **(C)** z direction. The positions correspoding to the ECR resonance are indicated with vertical red lines.

FIGURE 5
PANDORA's plasma characteristics; **(A)** 3D total density; **(B)** average energy. The contour of the ECR resonance is indicated in green.
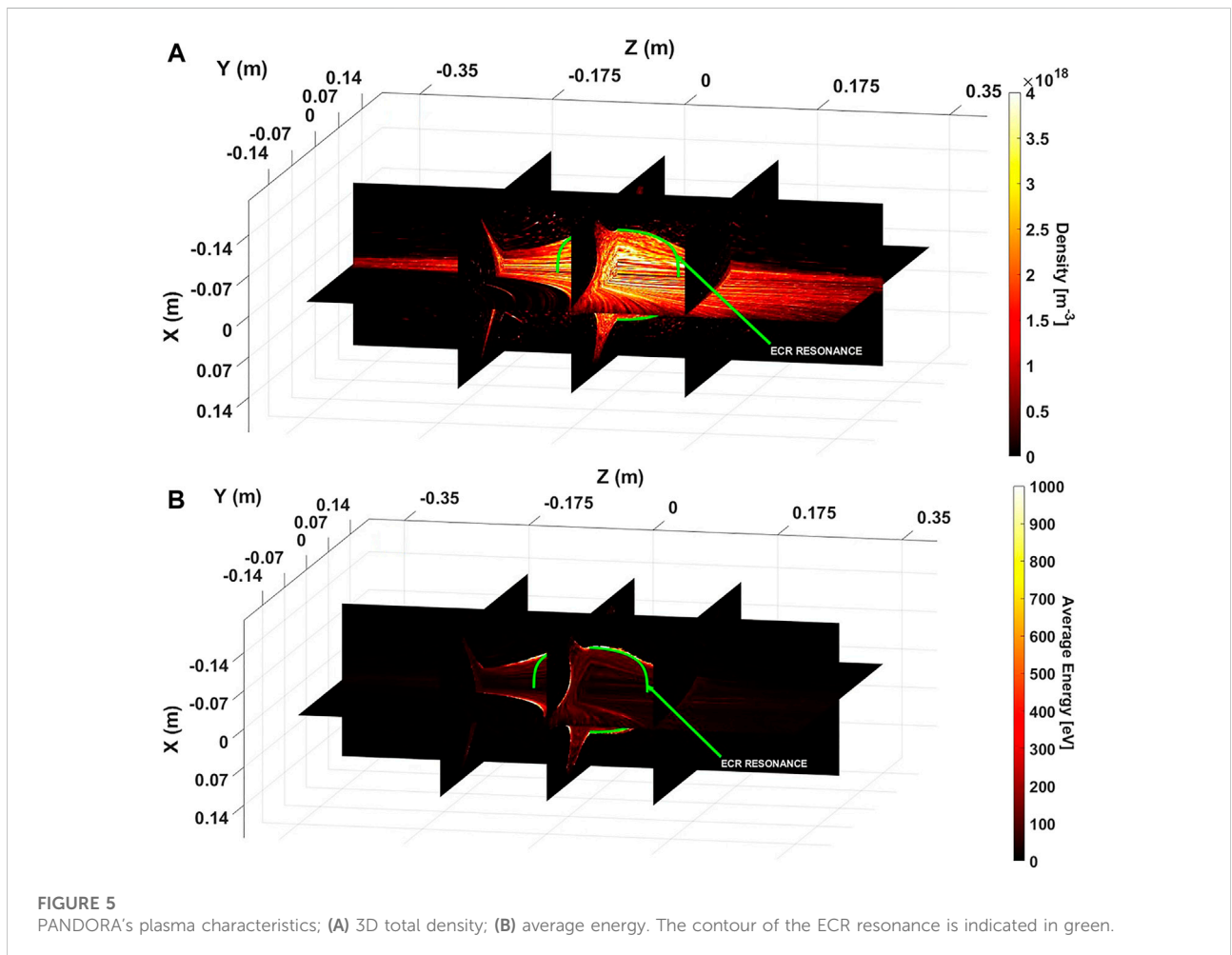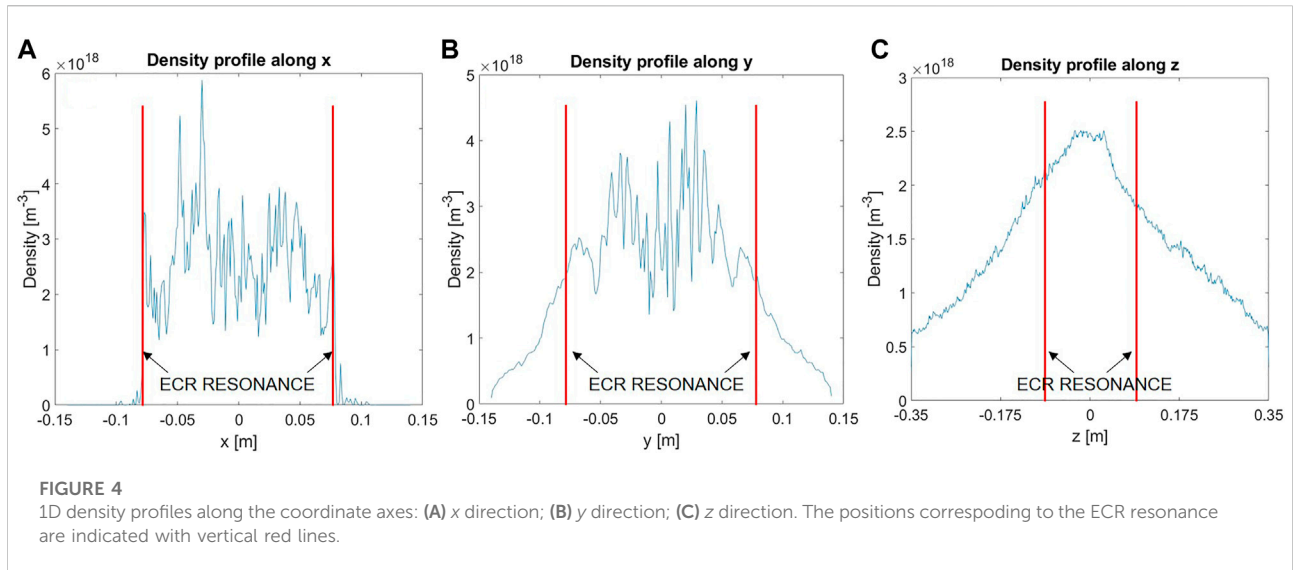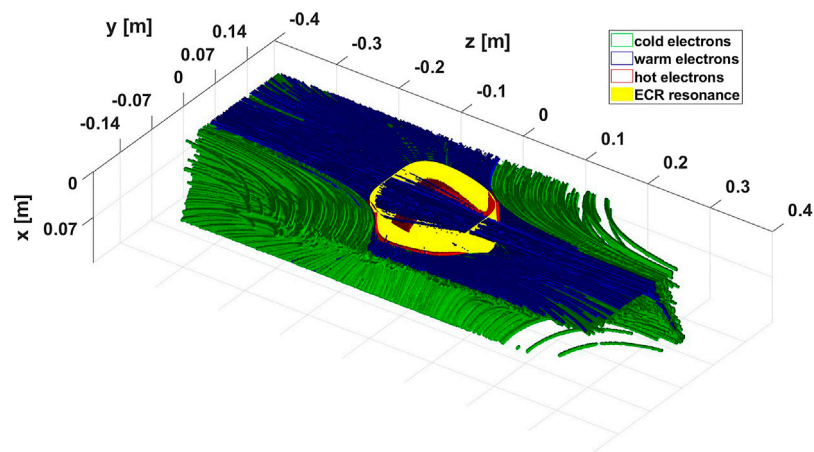
FIGURE 6
3D isosurfaces of the spatial distribution of the three electrons' populations: *cold* (green), *warm* (blue) and *hot* (red). The ECR resonance corresponds to the yellow surface.
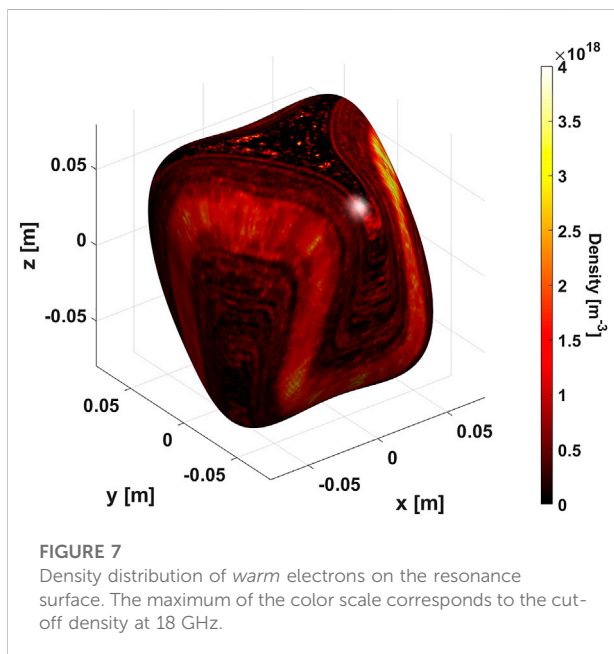
FIGURE 7
Density distribution of *warm* electrons on the resonance surface. The maximum of the color scale corresponds to the cut-off density at 18 GHz.

integration of the equation of motion, as well as to store the respective quantities in the occupation and energy accumulation maps. In the latest version of the code the electromagnetic field seen by each particle is the result of the superpositions of the values stored on the eight grid points surrounding its instantaneous position, using proper weights Birdsall and Langdon [17]. In the same way, occupation and energy accumulation maps are created distributing the relative quantities on the same grid points. A further improvement concerns the implementation of the relativistic Boris method, through a computationally more precise and faster formalism described in Zenitani and Umeda [20]. The results shown in the following section concerns the first application of the above-mentioned simulation scheme to a high volume, high frequency ECR plasma: even if the global convergence is not fully achieved yet, they already give relevant indications on the plasma density and energy distribution in such a new configuration and can still be considered satisfactory.

3 Simulations results

As mentioned in the previous section, the simulation domain is the cylindrical plasma chamber of the PANDORA trap, with a length of 700 mm, a radius of 140 mm and discretized in cells of 1 mm^3. Electromagnetic simulations were carried out at a frequency ν = 18 GHz and a power P_ν = 5 kW. The various steps of the self-consistent loop followed the evolution of 10^5 electrons, whose initial velocities were distributed according to a Maxwell-Boltzmann distribution with a temperature of 5 eV:

described in Figure 3: depending on the number of simulated particles, the integration step and time (of course besides the particular computer used) the calculations of a single step could last from one to several days.

In the previous version of the code Galatà et al. [13], the instantaneous position of a particle at each time step (x_{part}, y_{part}, z_{part}) was projected to the closest point of the 3D matrix reflecting the simulation domain, thus obtaining three indices (i, j, k): those indices were used to select the specific value of the electromagnetic field to be used in the

FIGURE 8
(A): distributon of warm electrons (blu) superimposed to the simulated point-like sources of γ emissions (green). **(B)**: cones of view of the 14 HPGe detectors (green) crossing the warm electrons distribution (blue).

considering all the characteristic times involved and in particular to describe properly the electrons' cyclotron motion, the integration step was chosen as $T_{step} = 10^{-12}$ s. To allow filling correctly the high energy part of the electrons' distribution as a consequence of the ECR resonance, the integration time was fixed to $T_{span} = 100$ μs: this translated in a total of 10^8 iterations. Following the scheme described in section 2, the self-consistent loop was iterated up to the Step3. ECR plasma electrons are usually grouped in three populations: *cold* electrons, characterized by a low kinetic energy, that constitute the bulk of the plasma; *warm* electrons, responsible for the ionization process; *hot* electrons, characterized by a very high kinetic energy, not involved in the ionization process, but that contribute considerably to the plasma self emission, especially in the hard X-rays region. By using the special routines implemented in the code, it was possible to create density and average energy maps for all the three electrons populations: we considered as *cold* those electrons with a kinetic energy $K \leq 100$ eV; *warm* those with $100 < K \leq 5000$ eV; finally, *hot* those with K > 5000 eV. In particular, the *warm* population is relevant for the scope of PANDORA, because its density and average energy will determine the charge state distribution set-up inside the plasma and will be used as a knob to experimentally verify its influence on the β-decay rate of several radionuclides (as expected by theoretical models).

Figure 4 shows the 1D total density profiles on both transversal planes (in the middle of the plasma chamber) and along the plasma chamber axis: it is worth noticing how the density reaches very high values, close to the cut-off density at the simulated frequency ($n_{cut-off} \sim 4 \cdot 10^{18}$ m^{-3}) and in some cases exceeding it. The asimmetry observed between the two transversal plane is a direct consequence of the asimmetry of the confining magnetic field, but especially along the *x* direction the formation of the so-called plasmoid/halo structure Ivanov and Wiesemann [21] is clearly visible.

Relevant information come from the distribution of the 3D total density and average energy: Figure 5 shows slice plots of both quantities. The colorbar of the density plot has been limited to the value corresponding to the cut-off density, in order to underline the fact that the PANDORA trap will create a very dense plasma, radially confined inside the resonance surface (whose contour is indicated in green) and with a density exceeding $n_{cut-off}$ in several locations. For what concerns the average energy, it reaches (and exceeds) 1 keV in the zones corresponding to the ECR resonance: if one considers that most of plasma electrons belong to the *cold* population, with a low kinetic energy, having such a high average energy is a clear indication of the creation of a huge amount of energetic electrons heated by the external microwave field.

It is interesting now to verify the distribution of electrons belonging to the three different populations: Figure 6 shows the isosurfaces corresponding to their spatial distributions, plotted in cut view for positive values of the *x* axis. It can be clearly seen how the three populations are nested one inside the other, going from the *cold* to the *hot* one: in particular, this last population is entirely distributed on (or in proximity of) the resonance surface (indicated in yellow), as a consequence of the extremely efficient energy transfer from the extern

microwave field to plasma electrons. The high energy reached makes the cross section for elastic scattering of those electrons very low, thus implying a very small diffusion away from the resonance zone.

It is important now to analyse a bit more in details the results concerning the *warm* population, being relevant for the scope of PANDORA. The first significant result comes from the relative abundance of this population with respect to the total number of electrons. In fact, by summing up the total occupation map and the one of *warm* electrons it has been observed that they constitute about the 20% of the total. This results is absolutely unprecedented, even for very high performances ECR sources (where the fraction of *warm* electrons is usually lower) and is most likely due to the optimum coupling of the external microwave field with the plasma chamber in the first place Mauro et al. [9], then with the plasma itself. Having such a high percentage of *warm* electrons will translate in very high charge states produced in the plasma, thus increasing the probability to detect significant variations of the half-lives of the radioactive species of interest. The optimum coupling of microwave can be deduced also by looking at Figure 7, showing the density distribution of *warm* electrons on the resonance surface, near which energetic electrons spend most of the time due to the confining effect of the ECR resonance Geller [4]. As for the case of Figure 5, the maximum of the color scale has been limited to the value corresponding to $n_{cut-off}$: it can be seen how the density is extremely high on this surface, reaching and exceeding $n_{cut-off}$ in some locations.

4 HPGe detectors position benchmark

With the aim of fulfilling the goal of the PANODRA project, the choice of the γ-detectors, their number and implementation on the magnetic trap is a key point. As described in section 1, 14 HPGe detectors will surround the plasma trap in order to detect as efficiently as possible the γ-rays accompanying the β-decay of the radionuclides of interest. The detectors will see the plasma through apertures made on the cryostat, that has been specially designed to void distorting the confining magnetic field Mauro et al. [9]. Given the dimension of the apertures, the particular orientation of the cones of view of the detectors will determine the amount of γs produced that will be effectively detected, depending on the particular portion of the plasma intercepted. In order to maximize the detection of the γs of interest, this portion should be part of the distribution of *warm* eletrons, where most of the ionisatons to high charge states take place. The evaluation of the detection efficiency, described in Naselli et al. [8], has been carried out by supposing γs being emitted isotropically from point-like sources filling an ellipsoidal volume having semi-axes of 79 mm, 79 and

56 mm (along, respectively, x, y and z) and resembling the resonance surface, thus obtaining the cones of view intercepted by the detectors. It is interesting now to superimpose those cones to the distribution of warm electrons obtained by the previously described numerical simulations: the results are shown in Figure 8. From part (A) it can be observed how the sources are completely internalised in the cloud of *warm* electrons, thus validating the model used to deduce the detection efficiency. Much more important is the information coming from part (B) of Figure 8: it can be clearly seen how the cones of view of the detectors intercept perfectly the *warm* electrons distribution, thus maximizing not only the probability to detect the γs accompanying the β-decay but also the possibility to observe variations of the half-life by tuning the charge state distribution as a consequence of a variation of the electrons energy.

5 Conclusions

In conclusion, the latest version of the developed self-consistent approach demonstrated its ability to describe correctly the anisotropic magnetoplasmas produced inside an ECR trap, even in the case of a high volume, high frequency model. The plasma produced within PANDORA will be characterized by an unprecedented fraction of *warm* electrons, thus increasing dramatically the ionization efficiency. This aspect, together with the possibility to vary dynamically the plasma parameters and the implementation of a set af multi-diagnostics, will allow to correlate any possible variation of the half-lives of β-decaying radioactive species to the plasma ionization state. The results of the numerical simulations allowed also to benchmark the choice of the specific orientation of the 14 HPGe detectors, demonstrating how the cones of view perfectly intercept the *warm* electrons spatial distribution: this means that they will point exactly where most of the ionizations will take place, thus increasing the detection sensitivity to variations of the in-plasma charge state distribution.

t, and intellectual contribution to the work and approved it for publication.

Data availability statement

The raw data supporting the conclusions of this article will be made available by the authors, without undue reservation.

Author contributions

AG developed the original code and implemented new features DM provided the background physics in relation with

PANDORA EN followed the part of the work connected with the gamma rays detection BM and AP carried out the necessary data analysis in the different electrons' energy ranges explored GT is in charge of the electromagnetic simulations.

Conflict of interest

The authors declare that the research was conducted in the absence of any commercial or financial relationships that could be construed as a potential conflict of interest.

Publisher's note

All claims expressed in this article are solely those of the authors and do not necessarily represent those of their affiliated organizations, or those of the publisher, the editors and the reviewers. Any product that may be evaluated in this article, or claim that may be made by its manufacturer, is not guaranteed or endorsed by the publisher.

References

1. Bosch F, Faestermann T, Friese J, Heine F, Kienle P, Wefers E, et al. Observation of bound-state β^- decay of fully ionized ^{187}Re: ^{187}Re–^{187}Os cosmochronometry. *Phys Rev Lett* (1996) 77:5190–3. doi:10.1103/PhysRevLett.77.5190

2. Jung M, Bosch F, Beckert K, Eickhoff H, Folger H, Franzke B, et al. First observation of bound-state β^- decay. *Phys Rev Lett* (1992) 69:2164–7. doi:10.1103/PhysRevLett.69.2164

3. Mascali D, Busso M, Mengoni A, Amaducci S, Castro G, Celona L, et al. The PANDORA project: An experimental setup for measuring in-plasma β-decays of astrophysical interest. *EPJ Web Conf* (2020) 227:01013. doi:10.1051/epjconf/202022701013

4. Geller R. *Electron cyclotron resonance ion sources and ECR plasmas*. Taylor & Francis (1996).

5. Naselli E, Rácz R, Biri S, Mazzaglia M, Galatà A, Celona L, et al. Quantitative analysis of an ECR ar plasma structure by x-ray spectroscopy at high spatial resolution. *J Instrum* (2022) 17(2022):C01009. doi:10.1088/1748-0221/17/01/c01009

6. Naselli E, Mascali D, Caliri C, Castro G, Celona L, Galatà A, et al. Nuclear β-decays in plasmas: How to correlate plasma density and temperature to the activity. *EPJ Web Conf* (2020) 227:02006. doi:10.1051/epjconf/202022702006

7. Agostinelli S, Allison J, Amako K, Apostolakis J, Araujo H, Arce P, et al. Geant4—A simulation toolkit. *Nucl Instr Methods Phys Res Section A: Acc Spectrometers, Detectors Associated Equipment* (2003) 506:250–303. doi:10.1016/S0168-9002(03)01368-8

8. Naselli E, Santonocito D, Amaducci S, Galatà A, Gaosduff A, Mauro GS, et al. *Frontiers in physics - research topics: Nuclear physics and Astrophysics in plasma traps (forthcoming)* (2022).Design study of a hpge detectors array for β-decays investigation in laboratory ecr plasmas

9. Mauro GS, Celona L, Torrisi G, Pidatella A, Naselli E, Russo F, et al. *Frontiers in physics - research topics: Nuclear physics and Astrophysics in plasma traps (forthcoming)* (2022).An innnovative superconducting magnetic trap for probing β-decay in plasmas

10. Torrisi G, Mascali D, Sorbello G, Neri L, Celona L, Castro G, et al. Full-wave fem simulations of electromagnetic waves in strongly magnetized non-homogeneous plasma. *J Electromagn Waves Appl* (2014) 28:1085–99. doi:10.1080/09205071.2014.905245

11. Mascali D, Torrisi G, Neri L, Sorbello G, Castro G, Celona L, et al. 3d-full wave and kinetics numerical modelling of electron cyclotron resonance ion sources plasma: Steps towards self-consistency. *Eur Phys J D* (2015) 69:27. doi:10.1140/epjd/e2014-50168-5

12. Galatà A, Mascali D, Neri L, Celona L. A new numerical description of the interaction of an ion beam with a magnetized plasma in an ECR-based charge breeding device. *Plasma Sourc Sci Technol* (2016) 25:045007. doi:10.1088/0963-0252/25/4/045007

13. Galatà A, Mascali D, Gallo CS, Torrisi G. Self-consistent modeling of beam-plasma interaction in the charge breeding optimization process. *Rev Scientific Instr* (2020) 91:013506. doi:10.1063/1.5130704

14. Galatà A, Mascali D, Neri L, Torrisi G, Celona L. A three-dimensional numerical modelling of the phoenix-spes charge breeder based on the Langevin formalism. *Rev Scientific Instr* (2016) 87:02B507. doi:10.1063/1.4935010

15. Galatà A, Mascali D, Torrisi G, Neri L, Celona L, Angot J. Influence of the injected beam parameters on the capture efficiency of an electron cyclotron resonance based charge breeder. *Phys Rev Accel Beams* (2017) 20:063401. doi:10.1103/PhysRevAccelBeams.20.063401

16. Mishra B, Pidatella A, Biri S, Galatà A, Naselli E, Rácz R, et al. A novel numerical tool to study electron energy distribution functions of spatially anisotropic and non-homogeneous ecr plasmas. *Phys Plasmas* (2021) 28:102509. doi:10.1063/5.0061368

17. Birdsall C, Langdon A. Plasma Physics via computer simulation. *Series in plasma physics and fluid dynamics*. Taylor & Francis (2004).

18. Manheimer WM, Lampe M, Joyce G. Langevin representation of coulomb collisions in pic simulations. *J Comput Phys* (1997) 138:563–84. doi:10.1006/jcph.1997.5834

19. MacDonald WM, Rosenbluth MN, Chuck W. Relaxation of a system of particles with coulomb interactions. *Phys Rev* (1957) 107:350–3. doi:10.1103/PhysRev.107.350

20. Zenitani S, Umeda T. On the boris solver in particle-in-cell simulation. *Phys Plasmas* (2018) 25:112110. doi:10.1063/1.5051077

21. Ivanov A, Wiesemann K. Ion confinement in electron cyclotron resonance ion sources (ecris): Importance of nonlinear plasma-wave interaction. *IEEE Trans Plasma Sci IEEE Nucl Plasma Sci Soc* (2005) 33:1743–62. doi:10.1109/TPS.2005.860078